Solubility and stability of barium arsenate and barium hydrogen arsenate at 25 °C

Yinian Zhu*, Xuehong Zhang, Qinglin Xie,
Yudao Chen, Dunqiu Wang, Yanpeng Liang, Jie Lu

*Department of Resources and Environmental Engineering, Guilin University of Technology,
Jian-Gan Road 12, Guilin 541004, Guangxi, China*

Abstract

The inconsistency among current thermodynamic data of $Ba_3(AsO_4)_2(c)$ and $BaHAsO_4 \cdot H_2O(c)$ led the authors to obtain independent solubility data of barium arsenate by both precipitation and dissolution experiments. Low and neutral pH (3.63–7.43) favored the formation of $BaHAsO_4 \cdot H_2O(c)$. Both $BaHAsO_4 \cdot H_2O(c)$ and $Ba_3(AsO_4)_2(c)$ formed at the neutral pH conditions (7.47, 7.66), whereas $Ba_3(AsO_4)_2(c)$ was the only solid phase precipitated at high pH (13.03, 13.10). The $Ba_3(AsO_4)_2(c)$ precipitate acquired at 50 °C appeared as small leafy crystal, while the $Ba_3(AsO_4)_2(c)$ solid precipitated at 25 °C comprised granular aggregate with some smaller crystal clusters. XRD and SEM analyses of $Ba_3(AsO_4)_2(c)$ and $BaHAsO_4 \cdot H_2O(c)$ indicated that the solids were indistinguishable before and after the dissolution experiments. In the present work, the solubility products (K_{sp}) for $Ba_3(AsO_4)_2(c)$ and $BaHAsO_4 \cdot H_2O(c)$ were determined to be $10^{-23.53}(10^{-23.01}$ to $10^{-24.00})$ and $10^{-5.60}(10^{-5.23}$ to $10^{-5.89})$, respectively. ΔG_f° for $Ba_3(AsO_4)_2(c)$ and $BaHAsO_4 \cdot H_2O(c)$ were calculated to be -3113.40 and -1544.47 kJ/mol, respectively. There was no difference between the solubility products of the leafy and the granular $Ba_3(AsO_4)_2(c)$ solids.
© 2004 Elsevier B.V. All rights reserved.

Keywords: Solubility products; Stability; Barium arsenate; Barium hydrogen arsenate

1. Introduction

The solubility of arsenic solids is of importance in public health, water treatment, and geochemistry. The ability to predict the fate and behaviour of arsenic in soils and waste-affected environments requires knowledge of the processes that control arsenic distribution between solid and solution phases. One process that may control soluble arsenic in aerated environments is the precipitation of metal arsenates. Due to its purported stability, barium arsenate has been suggested to control arsenic concentrations in fresh water and in solid waste leachates [1].

The results of the theoretical examination by Wagemann [2] suggested barium arsenate as the solid phase controlling

soluble arsenate concentration at typical freshwater barium ion activity. It was also determined that barium arsenate is stable over a wide range of Eh and alkaline pH conditions. Barium arsenate has also been suggested to control soluble arsenate in coal ash leachates [3]. Rai et al. [4] concluded that barium arsenate could exist in weathered fly ash and was predicted to be the least soluble metal arsenate. Based on the geochemical modeling of arsenic in the groundwater of the Rioverde basin, Mexico, Planer-Friedrich et al. [5] concluded that $Ba_3(AsO_4)_2$ is not likely to control arsenic concentrations at all rather than the mineral phase $BaHAsO_4 \cdot H_2O$ might be considered as the limiting mineral phase. In the same study, the PHREEQC software was used to model solution chemistry, which used the corrected solubility constants from Robins [6] and Essington [1].

The solubility of barium arsenate was first determined by Chukhlantsev [7]. The conditional solubility product

* Corresponding author. Tel.: +86 773 5895378; fax: +86 773 5897019.
E-mail address: zhuyinian@163.com (Y. Zhu).

constant $[Ba^{2+}]^3[AsO_4{}^{3-}]^2$, not corrected for ionic strength and determined at 20 °C, was calculated as 7.7×10^{-51} (log $K_{sp} = -50.11$). All thermodynamic data compilations that consider barium arsenate, principally geochemical model data bases, contain the stability product constant determined by Chukhlantsev [7], converted to zero ionic strength and 25 °C. However, Rai et al. [4] suspected the solubility product of barium arsenate to be wrong comparing it with those of Mg-arsenate (log $K_{sp} = -30.32$), Ca-arsenate (log $K_{sp} = -18.48$), and Sr-arsenate (log $K_{sp} = -18.79$). Although Robins [6] and Essington [1] concluded that the mineral phase is far less stable than previously assumed, there are still great differences among the available literature data. Chukhlantsev [7], Robins [6], Essington [1], Davis [8] and Orellana et al. [9] reported the solubility (log K_{sp}) of barium arsenate $[Ba_3(AsO_4)_2(c)]$ to be -50.11, -16.58, -21.62, -21.57, and -19.3, respectively. Further doubt was also placed on the validity of barium hydrogen arsenate solubility. Robins [6], Essington [1], Davis [8] and Orellana et al. [9] determined the solubility (log K_{sp}) of BaHAsO$_4\cdot$H$_2$O(c) to be -4.70, -24.64, $-3.86(-5.51)$ and -0.8, respectively.

Due to the inconsistency of the currently accepted solubility of barium arsenate, a study was undertaken to determine the solubility and stability of Ba$_3$(AsO$_4$)$_2$(c) and BaHAsO$_4\cdot$H$_2$O(c) by both precipitation and dissolution.

2. Experimental methods

2.1. Precipitation experiments

These experiments were made in HDPE bottles by mixing 30 ml CO$_2$-free 0.5 M Ba(ClO$_4$)$_2$ solution with 20 ml 0.5 M H$_3$AsO$_4$ solution, both of which were adjusted to a certain pH with KOH or HNO$_3$ solutions before mixing. The bottles were then sealed tightly to minimize intrusion of atmospheric CO$_2$, stored at 25 °C and periodically agitated. After reaction for more than 50 days, the pH values of the solutions were measured. Simultaneously, 10 ml samples were extracted from each bottle and centrifuged. The liquid fraction was filtered through a 0.20 μm filter into a vial, and then diluted and stabilized with 0.2% HNO$_3$ in 100 ml volumetric flasks. The concentrations of barium and arsenic were analyzed by atomic absorption spectrometer (Perkin-Elmer AAnalyst 700). The solid fractions were extracted via filtration, air-dried, and then characterized using an automated Brucker D8Advance X-ray diffractometer with Cu Kα X-ray radiation.

2.2. Dissolution experiments

2.2.1. Solid preparation and characterization

Barium arsenate [Ba$_3$(AsO$_4$)$_2$(c)] was precipitated by mixing a CO$_2$-free 0.2 M Ba(ClO$_4$)$_2$ solution, adjusted to pH 12 with KOH, with a 0.2 M H$_3$AsO$_4$ solution, also adjusted to pH 12 with KOH, in 3:2 Ba/As mole ratio proportions. The mixture was reacted at 25 and 50 °C for a 16 h period. The white precipitate was separated by filtration through a 0.2 μm syringe filter, washed with absolute ethanol, oven-dried at 110 °C for 24 h. The precipitate was characterized by X-ray diffraction and identified as Ba$_3$(AsO$_4$)$_2$(c). The morphology was analyzed by scanning electron microscopy (SEM, Joel JSM-5610LV).

BaHAsO$_4\cdot$H$_2$O(c) was made by mixing a CO$_2$-free 0.5 M Ba(ClO$_4$)$_2$ solution, adjusted to pH 6 with KOH, and a 0.5 M H$_3$AsO$_4$ solution, also adjusted to pH 6 with KOH, in 1:1 Ba/As mole ratio proportions. The mixture was reacted at 50 °C for a 16 h period. The white precipitate was separated, washed with absolute ethanol, oven-dried, and analyzed by X-ray diffraction. The results of X-ray diffraction analysis indicated that the solid precipitated was phase-pure BaHAsO$_4\cdot$H$_2$O(c). The morphology was analyzed by scanning electron microscopy (SEM, Joel JSM-5610LV).

2.2.2. Dissolution and equilibration

The solubility experiments were conducted in much the same manner as those used for determining the solubility of magnesite [MgCO$_3$] by Kittrick and Peryea [10] and for determining the solubility of barium arsenate by Essington [1]. The equilibrium solubility experiments were conducted under different ionic strength conditions. All equilibrium solubility systems were replicated at least three-fold.

One or 0.5 g samples of Ba$_3$(AsO$_4$)$_2$(c) or BaHAsO$_4\cdot$H$_2$O(c) were placed in 50 ml polypropylene bottles. An amount of 50 ml of either pure water or 0.1, 0.01, 0.001, 0.0001, 0.00001 M KOH solution was added to each bottle. The bottles were capped and placed in a temperature-controlled water bath (25 °C). The samples were equilibrated, with periodic shaking, for time periods varying from 30 to 50 days. During the dissolution of both Ba$_3$(AsO$_4$)$_2$ and BaHAsO$_4\cdot$H$_2$O in water, the solution pHs change with time. When the solutions have reached a state of equilibrium, their pHs should be stable. The solution pHs were periodically measured to monitor the equilibrium state. After 1 week reaction, the solution pHs had reached stable in this dissolution experiment.

After equilibration, the aqueous phase pH was determined and 10 ml samples were extracted from each bottle, centrifuged and filtered. The liquid fractions and the solid fractions were analyzed and characterized using AAS, XRD and SEM in the same manner as described in the previous precipitation experiments.

2.3. Simulation and calculation of experimental data using PHREEQC

Associated with each precipitation and dissolution experiment is an assemblage of solid phases, a solution phase containing dissolved barium and arsenic (which may also contain ClO$_4{}^-$, K$^+$ and NO$_3{}^-$), and a pH value. Assuming equilibrium has been reached, the values of these parameters can

Table 1
Equilibrium constants for the various aqueous species used by PHREEQC

Reaction	log K (25 °C)
$H_3AsO_4 = H_2AsO_4^- + H^+$	−2.243
$H_3AsO_4 = HAsO_4^{2-} + 2H^+$	−9.001
$H_3AsO_4 = AsO_4^{3-} + 3H^+$	−20.597
$Ba^{2+} + H_2O = BaOH^+ + H^+$	−13.358
$H_2O = OH^- + H^+$	−13.998

be calculated using established theoretical principles [11]. In this study, the simulations were performed using PHREEQC, a program based on the ion-association aqueous model. The input is free-format and uses order-independent keyword data blocks that facilitate the building of models that can simulate a wide variety of aqueous-based scenarios [12].

The aqueous species considered for total barium in the calculations were Ba^{2+} and $BaOH^+$. For total arsenate, the species considered were H_3AsO_4, $H_2AsO_4^-$, $HAsO_4^{2-}$ AsO_4^{3-}. Association constants for the soluble arsenate species are listed in Table 1.

Activity coefficients of aqueous species are defined with the extended Debye–Hückel equation:

$$\log \gamma_i = -\frac{A z_i^2 \sqrt{\mu}}{1 + B a_i^0 \sqrt{\mu}}, \quad \mu < 0.1 \, \text{mol/kg} \tag{1}$$

or the Davies equation

$$\log \gamma_i = -A z_i^2 \left(\frac{\sqrt{\mu}}{1 + \sqrt{\mu}} - 0.3\mu \right), \quad \mu < 0.5 \, \text{mol/kg} \tag{2}$$

or WATEQ Debye–Hückel equation:

$$\log \gamma_i = -\frac{A z_i^2 \sqrt{\mu}}{1 + B a_i^0 \sqrt{\mu}} + b_i \mu, \quad \mu < 1.0 \, \text{mol/kg} \tag{3}$$

where γ_i is the activity coefficient of aqueous specie i, z_i the ionic charge of aqueous species i, μ the ionic strength, A and B the constants dependent only on temperature, a_i^0 and b_i the ion-specific parameters. Unless otherwise specified in the database file or the input data set, the Davies equation is used for charged species. For uncharged species, the first term of the activity coefficient equation is zero, and the WATEQ Debye–Hückel equation reduces to the Setchenow equation ($\ln \gamma_i = b_i \mu$). Unless otherwise specified, b_i is assumed to be 0.1 for all uncharged species [12].

The chemical equilibrium computer model used to derive Ba^{2+}(aq) and AsO_4^{3-}(aq) activities calculated free ionic and ion pair species distribution by numerically solving a set of coupled nonlinear algebraic equations by successive iterations. Each equation relates total soluble element concentration to free ionic and ion pair species concentrations using the appropriate stability constants and stoichiometry. Soluble potassium arsenate and barium arsenate ion pairs (e.g., $KAsO_4^{2-}$, $KHAsO_4^-$, $BaAsO_4^-$, $BaHAsO_4^0$) were not considered in the calculations. Barium arsenate ion pair ΔG_f° values are not available in the literature. Wagman et al. [13] list ΔG_f° values of −1498.29, −1036.54,

and −1281.22 kJ/mol, for $K_3AsO_4^0$(aq), $KH_2AsO_4^0$(aq), and $K_2HAsO_4^0$(aq), respectively. However, as indicated by Essington [1], these values are simply the summation of the ΔG_f° values (taking into account the appropriate stoichiometries) of K^+(aq) (−283.26 kJ/mol), AsO_4^{3-}(aq) (−648.52 kJ/mol), $HAsO_4^{2-}$(aq) (−714.71 kJ/mol), and $H_2AsO_4^-$(aq) (−753.29 kJ/mol) from Wagman et al. [13,14].

3. Results

3.1. XRD and SEM analyses

3.1.1. Precipitation experiments

Previous work has shown that two barium-arsenic solids exist [1,6]. Dominance of the $HAsO_4^{2-}$ species (over AsO_4^{3-}) at circa neutral pHs favored the formation of the $BaHAsO_4 \cdot H_2O$(c) solid over $Ba_3(AsO_4)_2$(c). Some data indicated the possibility of a mixed system under the higher alkaline pH conditions (where both $BaHAsO_4 \cdot H_2O$(c) and $Ba_3(AsO_4)_2$(c) solids were present). However, the $Ba_3(AsO_4)_2$(c) solid appeared to be the phase to precipitate at high pH. XRD analyses of ten separate precipitation experiments revealed that $BaHAsO_4 \cdot H_2O$(c) precipitated within the pH range of 3.63–7.43. A mixture of $Ba_3(AsO_4)_2$(c) and $BaHAsO_4 \cdot H_2O$(c) precipitated between pH of 7.47–7.66. $Ba_3(AsO_4)_2$(c) was the sole solid phase precipitated at high pH (13.03 or 13.10) (Fig. 1).

3.1.2. Dissolution experiments

X-ray diffraction of $Ba_3(AsO_4)_2$(c) was performed on the solids "before" and "after" the dissolution experiments. As illustrated in Fig. 2, the results of the XRD analyses before dissolution were indistinguishable from those after dissolution.
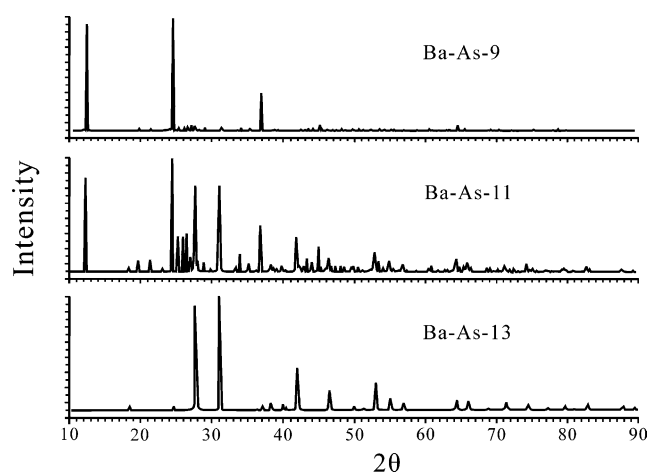

Fig. 1. X-ray diffraction analysis of the reaction products precipitated from mixing 30 ml 0.5 M $Ba(ClO_4)_2$ solution with 20 ml 0.5 M H_3AsO_4 solution. The solid Ba-As-9 precipitated at pH 7.43 has a typical pattern of $BaHAsO_4 \cdot H_2O$(c); the solid Ba-As-11 precipitated at pH 7.66 was a mixture of $Ba_3(AsO_4)_2$(c) and $BaHAsO_4 \cdot H_2O$(c); the solid Ba-As-13 precipitated at pH 13.10 was pure $Ba_3(AsO_4)_2$(c).

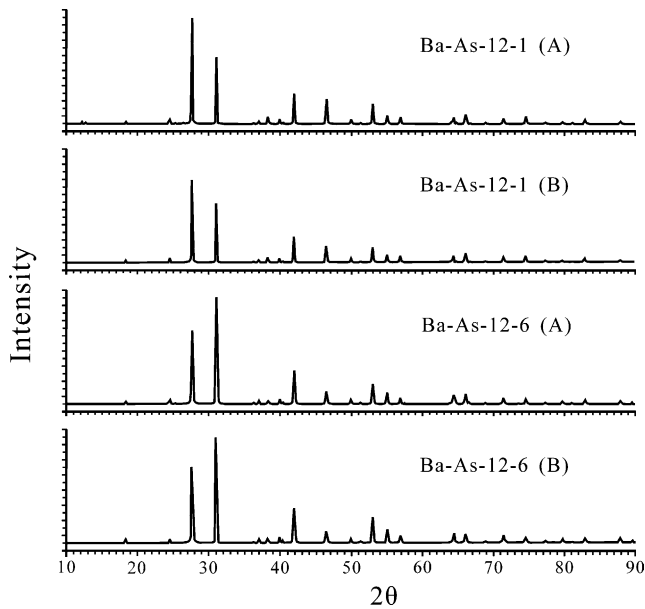Fig. 2. X-ray diffraction analysis of barium arsenate solids $Ba_3(AsO_4)_2(c)$. (A) Solid analysis before solubility experiments; (B) solid analysis after solubility experiments. The solid Ba-As-12-6 was precipitated at 25 °C and the solid Ba-As-12-1 was synthesized at 50 °C.

Morphological analysis of the $Ba_3(AsO_4)_2(c)$ precipitate was performed by scanning electron microscopy (SEM), before and after the dissolution experiments (Figs. 3 and 4). The results showed that the form of the $Ba_3(AsO_4)_2(c)$ crystal was related to their precipitation temperature. The $Ba_3(AsO_4)_2(c)$ precipitate acquired at 50 °C comprised smaller leafy crystal (1–5 μm diameter). In contrast, the $Ba_3(AsO_4)_2(c)$ solid precipitated at 25 °C existed mainly as granular aggregate (Rhombohedral grain: 20–100 μm diameter) with some smaller crystal clusters. After the equilibration period at 25 °C, the morphology of the two crystals did not change, for both leafy and grain type $Ba_3(AsO_4)_2(c)$ samples.

XRD and SEM analyses were also performed on the $BaHAsO_4·H_2O(c)$ solids before and after the dissolution experiments. As illustrated in Fig. 5, the results of the XRD

analyses on materials before reaction were indistinguishable from those following the equilibrium reaction. The $BaHAsO_4·H_2O(c)$ particles were observed by SEM to be well sorted and composed of numerous trigonal (hexagonal) plates (Fig. 6). The $BaHAsO_4·H_2O(c)$ solid prior to dissolution comprised large platy crystal (10–50 μm diameter), but which became smaller after the 50 days dissolution experiment was initiated (<10 μm diameter).

3.2. Solubility of barium arsenate $[Ba_3(AsO_4)_2(c)]$

The dissolution of $Ba_3(AsO_4)_2(c)$ can be described in the same manner as Essington by the following reaction [1]:

$$Ba_3(AsO_4)_2(c) = 3Ba^{2+}(aq) + 2AsO_4^{3-}(aq) \qquad (4)$$
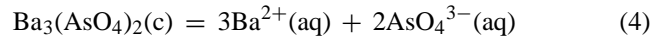
Assuming unit activity of the solid phase

$$K_{sp} = (Ba^{2+})^3(AsO_4^{3-})^2 \qquad (5)$$

where (·) denotes thermodynamic activity of the species enclosed and K_{sp} the equilibrium constant of dissolution for Eq. (4).

The standard free energy of reaction (ΔG_r°), in kJ/mol, is related to K_{sp} at standard temperature (298.15 K) and pressure (0.101 MPa) by

$$\Delta G_r^\circ = -5.708 \log K_{sp} \qquad (6)$$

For Eq. (4),

$$\Delta G_r^\circ = 3\Delta G_f^\circ[Ba^{2+}] + 2\Delta G_f^\circ[AsO_4^{3-}] \\ - \Delta G_f^\circ[Ba_3(AsO_4)_2(c)] \qquad (7)$$

Rearranging,

$$\Delta G_f^\circ[Ba_3(AsO_4)_2(c)] = 3\Delta G_f^\circ[Ba^{2+}] \\ + 2\Delta G_f^\circ[AsO_4^{3-}] - \Delta G_r^\circ \qquad (8)$$

The solution chemistry representing equilibrium involving the solution phase and $Ba_3(AsO_4)_2(c)$, along with the calculated $\log K_{sp}$ using PHREEQC, are shown in Table 2.

Fig. 3. The SEM analysis of $Ba_3(AsO_4)_2(c)$ where (A) shows the solid prior to the solubility experiments and (B) shows the solid after the 42 days equilibrium. The $Ba_3(AsO_4)_2(c)$ solid used in the dissolution experiments was obtained at 50 °C.
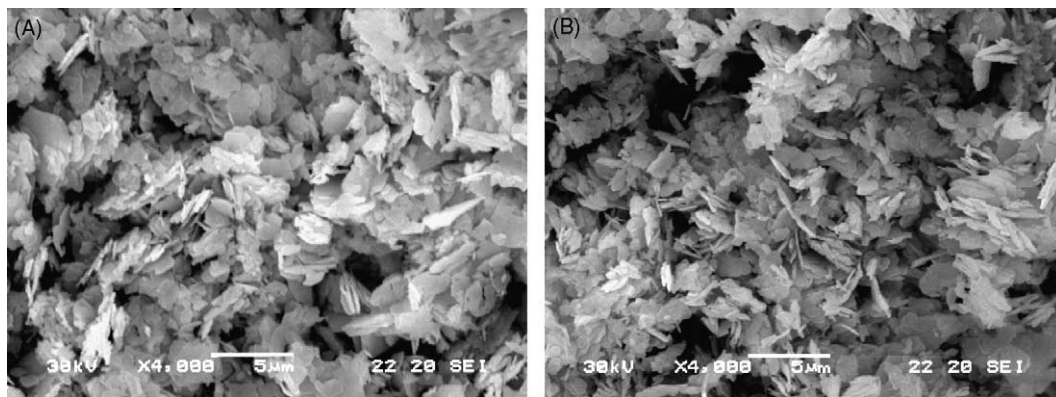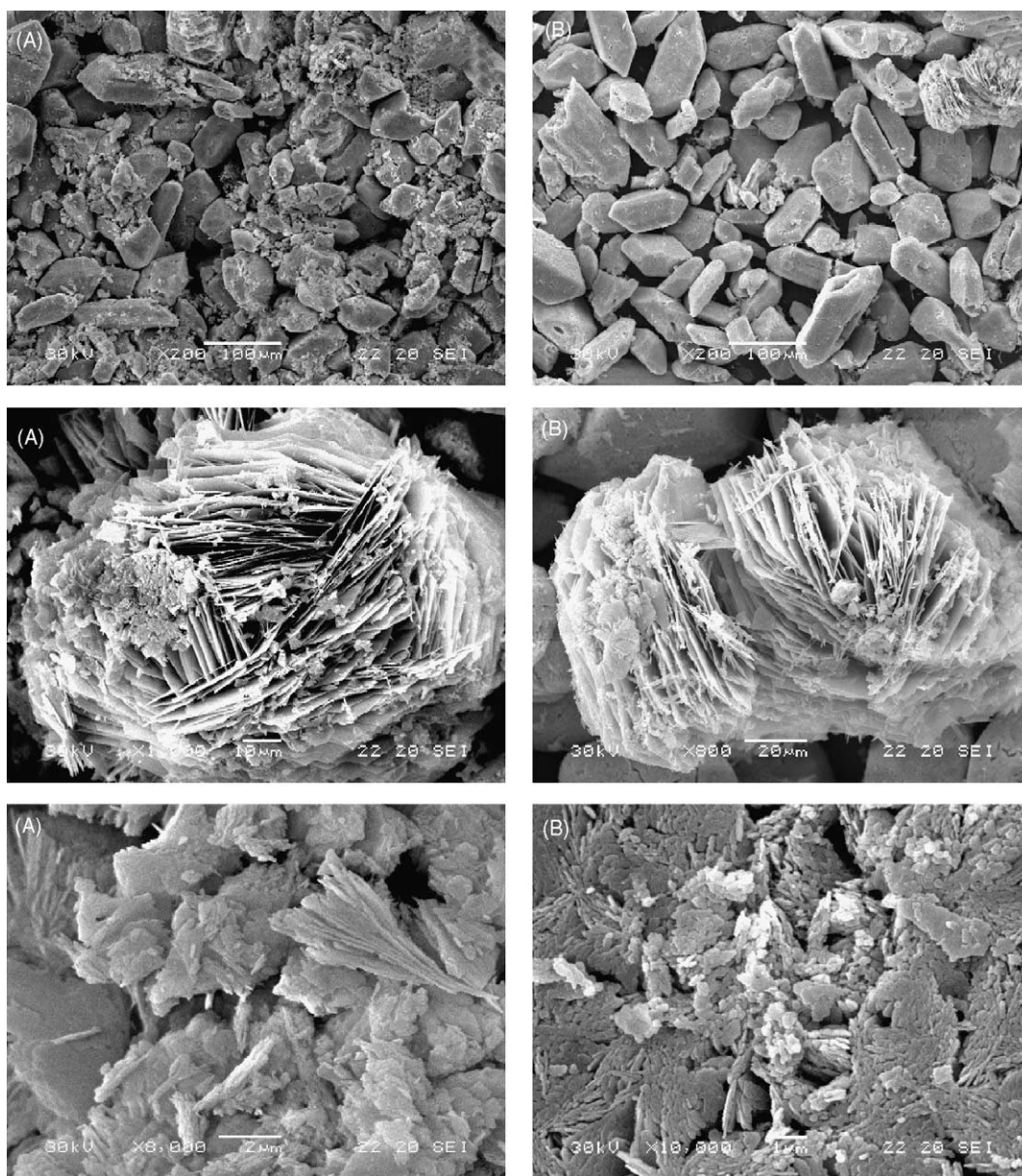
Fig. 4. The SEM analysis of $Ba_3(AsO_4)_2$(c) where (A) shows the solid prior to the solubility experiments and (B) shows the solid after the 30 days equilibrium. The $Ba_3(AsO_4)_2$(c) solid used in the dissolution experiments was obtained at 25 °C.
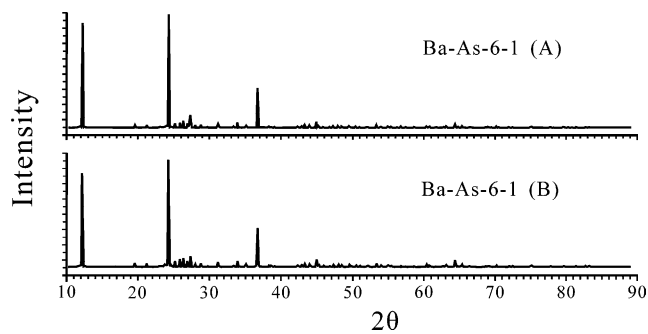

Fig. 5. X-ray diffraction analysis of barium hydrogen arsenate solids $BaHAsO_4·H_2O$(c). (A) Solid analysis before solubility experiments; (B) solid analysis after solubility experiments.

The arsenate concentration associated with the precipitation experiments was somewhat higher than that of the dissolution experiments. This may have been due to a little over-saturation of the aqueous solution with respect to $Ba_3(AsO_4)_2$(c) at higher pH.

The $\log K_{sp}$ of -23.53 (-23.01 to -24.00) was the mean obtained by averaging over all dissolution experiments at different pH values between 7.88 and 12.50 with reaction times of 30 days and greater. The values from the precipitation experiments at high ionic strengths (>1.0 M) were not used for this calculation. As the data illustrate, there was a high degree of consistency among the calculated $\log K_{sp}$ values under the experimental conditions imposed by the present study. The $\log K_{sp}$ values for the platy $Ba_3(AsO_4)_2$(c) solid
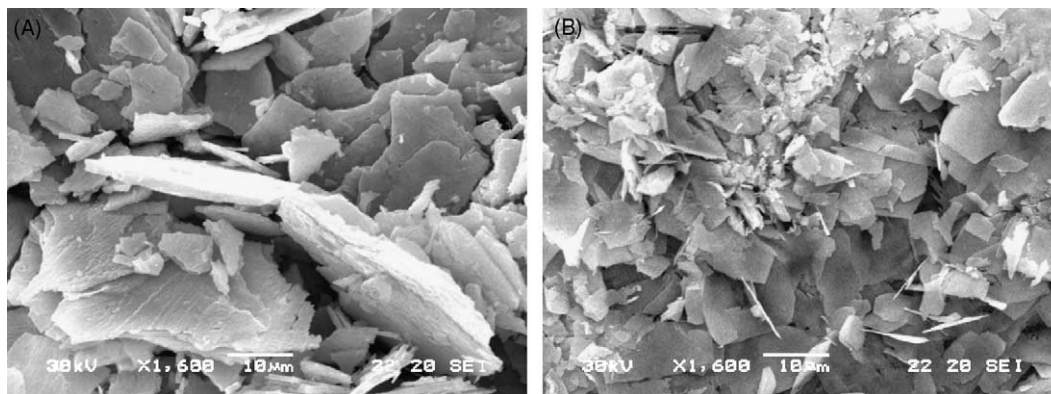
Fig. 6. The SEM analysis of BaHAsO$_4$·H$_2$O(c) where (A) shows the solid prior to the solubility experiments and (B) shows the solid after the 50 days equilibrium.

(Table 2: Ba-As-12-1–Ba-As-12-5) were in good agreement with those of the granular Ba$_3$(AsO$_4$)$_2$(c) solid.

Difference exists between our data and those available in the literature. The solubility product calculated for barium arsenate ($10^{-23.53}$ at 25 °C) is approximately 26.58 log units higher than $10^{-50.11}$ reported by Chukhlantsev [7] and approximately 6.95 log units lower than $10^{-16.58}$ reported by Robins [6]. But our solubility measurements for crystalline Ba$_3$(AsO$_4$)$_2$(c) are almost in agreement with those of Essington [1] and Davis [8] ($10^{-21.62}$ and $10^{-21.57}$, respectively).

The solubility of barium arsenate was first determined by Chukhlantsev [7] and widely used by subsequent researchers.

Their solutions, however, was analyzed only for Ba^{2+}; the solubility product of barium arsenate was obviously too low, when comparing it with those of Mg-arsenate, Ca-arsenate, and Sr-arsenate. The works of Essington [1] and Davis [8] are much more reliable than others. Based on our experimental results and those available in the literature, the solubility product of barium arsenate should be 10^{-21} to 10^{-24}. The results of our investigation indicated that Ba$_3$(AsO$_4$)$_2$(c) is significantly less stable than previously considered based on the results of Chukhlantsev [7]. Ba$_3$(AsO$_4$)$_2$(c) may not control soluble arsenic concentrations in natural or waste-affected environments as previously suggested [2,3,15].

Table 2
Analytical data and solubility determination of Ba$_3$(AsO$_4$)$_2$(c) at 25 °C

Sample number	Reacted time (days)	Final pH	Analytical concentration (mol/l)			log K_{sp}
			K^{+a}	Ba	As	
Ba-As-10	57 precipitation	7.47	0.3888	0.050521	0.000614	−21.46
Ba-As-11		7.66	0.4412	0.012139	0.001380	−22.11
Ba-As-12		13.03	0.5336	0.000042	0.028630	−20.64
Ba-As-13		13.10	0.8758	0.000034	0.034770	−20.84
Ba-As-12-1	42 dissolution	12.48	0.1000	0.000018	0.000937	−23.34
Ba-As-12-2		12.49	0.1000	0.000025	0.000751	−23.05
Ba-As-12-3		12.49	0.1000	0.000019	0.000782	−23.38
Ba-As-12-4		12.50	0.1000	0.000019	0.000728	−23.46
Ba-As-12-5		12.50	0.1000	0.000018	0.000764	−23.48
Ba-As-12-6	30 dissolution	12.50	0.1000	0.000042	0.000364	−23.01
Ba-As-12-7		12.51	0.1000	0.000041	0.000379	−23.03
Ba-As-12-8		12.51	0.1000	0.000039	0.000348	−23.14
Ba-As-11-1	38 dissolution	11.61	0.0100	0.000006	0.000533	−23.97
Ba-As-11-2		12.09	0.0100	0.000010	0.000483	−23.39
Ba-As-11-3		12.10	0.0100	0.000010	0.000544	−23.31
Ba-As-10-1		9.00	0.0010	0.000247	0.000204	−23.81
Ba-As-10-2		8.81	0.0010	0.000320	0.000204	−23.87
Ba-As-10-3		8.78	0.0010	0.000318	0.000218	−23.88
Ba-As-9-1		8.18	0.00010	0.000431	0.000715	−23.75
Ba-As-9-2		8.24	0.00010	0.000452	0.000862	−23.43
Ba-As-9-3		8.32	0.00010	0.000423	0.000576	−23.65
Ba-As-8-1		7.88	0.000010	0.000464	0.001055	−23.99
Ba-As-8-2		7.96	0.000010	0.000418	0.000993	−24.00
Ba-As-8-3		8.09	0.000010	0.000440	0.001013	−23.65

[a] Calculated from original concentration.

Table 3
Analytical data and solubility determination of BaHAsO$_4$·H$_2$O(c) at 25 °C

Sample number	Reacted time (days)	Final pH	Analytical concentration (mol/l)				log K_{sp}
			K^{+a}	NO$_3^{-a}$	Ba	As	
Ba-As-4	57 precipitation	3.62	0.1832		0.247579	0.151305	−5.40
Ba-As-5		3.69	0.1977		0.110027	0.136543	−5.66
Ba-As-6		3.63	0.2379		0.206947	0.062052	−5.84
Ba-As-7		4.15	0.3055		0.110391	0.039948	−5.73
Ba-As-8		5.45	0.3417		0.052385	0.008283	−5.44
Ba-As-9		7.43	0.3700		0.042438	0.001925	−5.23
Ba-As-10		7.47	0.3888		0.050521	0.000614	−5.67
Ba-As-11		7.66	0.4412		0.012139	0.001380	−5.89
Mix-1-2	54 precipitation	7.47	0.2375		0.010027	0.003202	−5.49
Mix-1-3		7.38	0.2375		0.006233	0.003121	−5.70
Mix-2-1		4.30	0.1260		0.073473	0.076240	−5.41
Mix-2-2		3.72	0.3264	0.0002	0.111993	0.111993	−5.73
Ba-As-6-1	50 dissolution	6.24		0.0020	0.004236	0.005750	−5.57
Ba-As-6-2		6.30		0.0024	0.004236	0.005978	−5.51
Ba-As-6-3		6.38		0.0008	0.004121	0.003466	−5.68
Ba-As-6-4		6.52		0.0016	0.003754	0.004198	−5.56
Ba-As-6-5		5.99		0.0008	0.005880	0.006909	−5.55
Ba-As-6-6		7.69			0.002030	0.002140	−5.74

^{a} Calculated from original concentration.

A ΔG_f°[Ba$_3$(AsO$_4$)$_2$(c)] of −3113.40 kJ/mol was calculated using Eqs. (6)–(8). This value is 151.8 kJ/mol more positive than −3265.2 kJ/mol calculated by Rai et al. [15] from the solubility data of Chukhlantsev [7]. Further, the ΔG_f° value determined in the present study is 41.06 kJ/mol more negative than the value determined from the data of Robins [6] and 12.2 kJ/mol more negative than the value estimated by Essington [1] (−3072.34 and −3101.2 kJ/mol, respectively).

3.3. Solubility of barium hydrogen arsenate [BaHAsO$_4$·H$_2$O(c)]

The dissolution of BaHAsO$_4$·H$_2$O(c) can be described by the following reaction:

$$BaHAsO_4 \cdot H_2O(c) = Ba^{2+}(aq) + HAsO_4^{2-}(aq) + H_2O \tag{9}$$
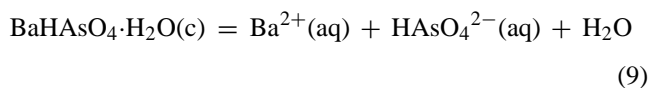
Assuming unit activity of the solid phase

$$K_{sp} = (Ba^{2+})(HAsO_4^{2-}) \tag{10}$$

where (·) denotes thermodynamic activity of the species enclosed and K_{sp} the equilibrium constant of dissolution for Eq. (9).

The standard free energy of reaction (ΔG_r°), in kJ/mol, is related to K_{sp} at standard temperature (298.15 K) and pressure (0.101 MPa) by Eq. (6).

For Eq. (9)

$$\Delta G_r^\circ = \Delta G_f^\circ[Ba^{2+}] + \Delta G_f^\circ[HAsO_4^{2-}] + \Delta G_f^\circ[H_2O]$$
$$- \Delta G_f^\circ[BaHAsO_4 \cdot H_2O(c)] \tag{11}$$

Rearranging, the ΔG_f°[BaHAsO$_4$·H$_2$O(c)] value was calculated as

$$\Delta G_f^\circ[BaHAsO_4 \cdot H_2O(c)] = \Delta G_f^\circ[Ba^{2+}]$$
$$+ \Delta G_f^\circ[HAsO_4^{2-}]$$
$$+ \Delta G_f^\circ[H_2O] - \Delta G_r^\circ \tag{12}$$

Table 3 gives the observed Ba and As concentrations as a function of the pH, together with K$^+$ and NO$_3^-$ concentrations. The log K_{sp} were calculated by using PHREEQC as described previously. The results of the precipitation experiments are in good accordance with those of the dissolution experiments. This indicates solution equilibrium with respect to BaHAsO$_4$·H$_2$O(c) and lends support to the significance of the calculated K_{sp} value.

BaHAsO$_4$·H$_2$O(c) was determined to be very soluble with a calculated mean K_{sp} value of 10$^{-5.60}$(10$^{-5.23}$ to 10$^{-5.89}$) using data from both precipitation and dissolution experiments. This value is approximately 19.04 log units higher than 10$^{-24.64}$ reported by Essington [1] and approximately 4.8 log units lower than 10$^{-0.8}$ reported by Orellana et al. [9], but in accordance with those of Robins [6] and Davis [8] (10$^{-4.70}$ and 10$^{-5.51}$, respectively).

Essington [1] determined the solubility of BaHAsO$_4$·H$_2$O(c) based not on his own experimental measurement, but on the data of Chukhlantsev [7] for Ba$_3$(AsO$_4$)$_2$(c). The solubility product $K_{sp} = 10^{-24.64}$ for BaHAsO$_4$·H$_2$O(c) resulted from his reevaluation was 3.02 log units lower than that for Ba$_3$(AsO$_4$)$_2$(c) (10$^{-21.62}$), which meant that BaHAsO$_4$·H$_2$O(c) was less soluble than Ba$_3$(AsO$_4$)$_2$(c). So, this result for BaHAsO$_4$·H$_2$O(c) was not reasonable and not reliable. The solubility product $K_{sp} = 10^{-0.8}$ for BaHAsO$_4$·H$_2$O(c) reported by Orellana

et al. [9] was higher than those calculated from both precipitation and dissolution [6,8, this work]. That study determined the solubility product only from precipitation experiments. The aqueous solution might not have reached equilibrium and was still supersaturated with regard to the solid. Based on our experimental results and those available in the literature, the solubility product for $BaHAsO_4 \cdot H_2O(c)$ varied between $10^{-4.5}$ and $10^{-6.0}$.

The experimentally observed K_{sp} value ($10^{-5.60}$) was used to calculate the free energy of formation of $BaHAsO_4 \cdot H_2O(c)$. The value of ΔG_f° for $BaHAsO_4 \cdot H_2O(c)$ is computed as -1544.47 kJ/mol by assuming ΔG_f° for $Ba^{2+} = -560.77$ kJ/mol, ΔG_f° for $HAsO_4^{2-} = -714.59$ kJ/mol and ΔG_f° for $H_2O = -237.141$ kJ/mol.

4. Conclusions

The mineral phase $Ba_3(AsO_4)_2(c)$ is far less stable than previously assumed by Chukhlantsev [7]. Although doubt was placed on the validity of barium arsenate solubility by Robins [6] and Essington [1], nothing has been changed in the geochemical databases to date. Further literature study and this work revealed also that Essington's solubility product for $BaHAsO_4 \cdot H_2O(c)$ ($K_{sp} = 10^{-24.64}$) to be wrong. $BaHAsO_4 \cdot H_2O(c)$ exists at low pH and is much more soluble than $Ba_3(AsO_4)_2(c)$.

Low pH favored the formation of $BaHAsO_4 \cdot H_2O(c)$, whereas both $BaHAsO_4 \cdot H_2O(c)$ and $Ba_3(AsO_4)_2(c)$ were stable at the neutral pH conditions, $Ba_3(AsO_4)_2(c)$ was the only solid phase precipitated at high pH.

XRD analyses of $Ba_3(AsO_4)_2(c)$ and $BaHAsO_4 \cdot H_2O(c)$ indicated that the solids were indistinguishable before and after the dissolution experiments. The $BaHAsO_4 \cdot H_2O(c)$ particles observed by SEM were well sorted and composed of numerous trigonal plates. The $Ba_3(AsO_4)_2(c)$ precipitate acquired at $50\,^\circ C$ appeared as small leafy crystal, while the $Ba_3(AsO_4)_2(c)$ solid precipitated at $25\,^\circ C$ existed mainly as granular aggregate with some smaller crystal clusters. There was no difference between the solubility products of the leafy and the granular $Ba_3(AsO_4)_2(c)$ solid in the dissolution experiments.

The solubility products for $Ba_3(AsO_4)_2(c)$ and $BaHAsO_4 \cdot H_2O(c)$ were verified by both precipitation and dissolution experiments to be $10^{-23.53}$($10^{-23.01}$ to $10^{-24.00}$) and $10^{-5.60}$($10^{-5.23}$ to $10^{-5.89}$), respectively. ΔG_f° values for $Ba_3(AsO_4)_2(c)$ and $BaHAsO_4 \cdot H_2O(c)$ were calculated to be -3113.40 and -1544.47 kJ/mol, respectively. The results indicated that barium-arsenic compounds are unlikely to form under natural conditions in drinking water sources and to control arsenic solubility as previously suggested. In comparison with calcium and magnesium arsenates, barium arsenate offers little advantage for removing arsenic as a stable and highly insoluble material.

References

[1] M.E. Essington, Soil Sci. Soc. Am. J. 52 (1988) 1566.
[2] R. Wagemann, Water Res. 12 (1978) 139.
[3] T.R. Turner, Environ. Sci. Technol. 15 (1981) 1062.
[4] D. Rai, J.M. Zachara, A.P. Schwab, R.L. Schmidt, D.C. Gavin, J.E. Rogers, EPRI Rep. EA-3356, Electric Power Res. Inst., Palo Alto, CA, 1984.
[5] B. Planer-Friedrich, M.A. Armienta, B.J. Merkel, Environ. Geol. 40 (2001) 1290.
[6] R.G. Robins, Metall. Trans. 16B (1985) 404.
[7] V. Chukhlantsev, J. Inorg. Chem. (USSR) 1 (1956) 1975.
[8] J. Davis, Pract. Period. Hazard., Toxic Radioact. Waste Manage. 4 (2000) 31.
[9] F. Orellana, E. Ahumada, C. Suarez, G. Cote, H. Lizama, Bol. Soc. Chil. Quim. 45 (2000) 415.
[10] J.A. Kittrick, F.J. Peryea, Soil Sci. Soc. Am. J. 50 (1986) 243.
[11] J.V. Bothe, P.W. Brown, J. Hazard. Mater. B 69 (1999) 197.
[12] D.L. Parkhurst, C.A.J. Appelo, U.S. Geological Survey, Water-Resources Investigations Report 99-4259, 1999.
[13] D.D. Wagman, W.H. Evans, V.B. Parker, R.H. Schumm, R.L. Nuttall, Natl. Bureau of Standards Tech. Note (U.S.) 270-8, 1981.
[14] D.D. Wagman, W.H. Evans, V.B. Parker, I. Harlow, S.M. Bailey, R.H. Schumm, Natl. Bureau of Standards Tech. Note (U.S.) 270-3, 1968.
[15] D. Rai, C.C. Ainsworth, L.E. Eary, S.V. Mattigod, D.R. Jackson, EPRI Rep. EA-5176, Electric Power Res. Inst., Palo Alto, CA, 1987.